Chapter 3: Cyclic Pyrrole–Imidazole Polyamides Targeted to the

Androgen Response Element

The text of this chapter was taken in part from a manuscript coauthored with Daniel A. Harki, John W. Phillips, Christian Dose, and Peter B. Dervan* (Caltech)

(Chenoweth, D.M., Harki, D.A., Phillips, J.W., Dose, C., Dervan, P. B. *J. Am. Chem. Soc.* **2009** In Press)

Abstract

Hairpin pyrrole–imidazole (Py-Im) polyamides are a class of cell-permeable DNA-binding small molecules that can disrupt transcription factor–DNA binding and regulate endogenous gene expression. The covalent linkage of antiparallel Py-Im ring pairs with an γ-amino acid turn unit affords the classical hairpin Py-Im polyamide structure. Closing the hairpin with a second turn unit yields a cyclic polyamide, a lesser-studied architecture mainly attributable to synthetic inaccessibility. We have applied our methodology for solution-phase polyamide synthesis to cyclic polyamides with an improved high-yield cyclization step. Cyclic 8-ring Py-Im polyamides **1–3** targets the DNA sequence 5'-WGWWCW-3' which corresponds to the androgen response element (ARE) bound by the androgen receptor transcription factor to modulate gene expression. We find that cyclic Py-Im polyamides **1–3** bind DNA with exceptionally high affinities and regulate the expression of AR target genes in cell culture studies, from which we infer that the cycle is cell permeable.

3.1 Introduction

Modulating the expression of eukaryotic gene networks by small molecules is a challenge at the frontier of chemical biology. Pyrrole–imidazole polyamides are a class of cell-permeable small molecules that bind to the minor groove of DNA in a sequence-specific manner.[1,2] Side-by-side stacked *N*-methylpyrrole (Py) and *N*-methylimidazole (Im) carboxamides (Im/Py pairs) distinguish G•C from C•G base pairs, whereas Py/Py pairs specify for both T•A and A•T.[3] Py-Im hairpin polyamides have been programmed for a broad repertoire of DNA sequences with affinities similar to endogenous transcription factors.[4] They are cell permeable and influence gene transcription by disrupting protein–DNA interfaces.[2,5,6] Hairpin polyamide interference of DNA binding by transcription factors such as HIF-1α,[7] androgen receptor (AR),[8] and AP-1[9] has been described in recent years, yielding a new approach toward gene control by small molecules.

In parallel with our gene regulation studies, a significant effort has been devoted to maximizing the biological potency of hairpin Py-Im polyamides through structural modifications. In particular, we have recently demonstrated that hairpin polyamides bearing the (*R*)-β-amino-γ-turn, such as polyamide **4**, possess favorable binding affinities to DNA and are useful in gene regulation studies (Figure 3.1).[5g] A significant effort exists in our laboratory to regulate aberrant AR-activated gene expression in prostate cancer.[8] To further optimize lead oligomer **4,** it would seem reasonable that closing the hairpin with an identical linker, yielding a cyclic structure **1**, would further enhance DNA affinity (Figure 3.1). Previous syntheses of cyclic polyamides using
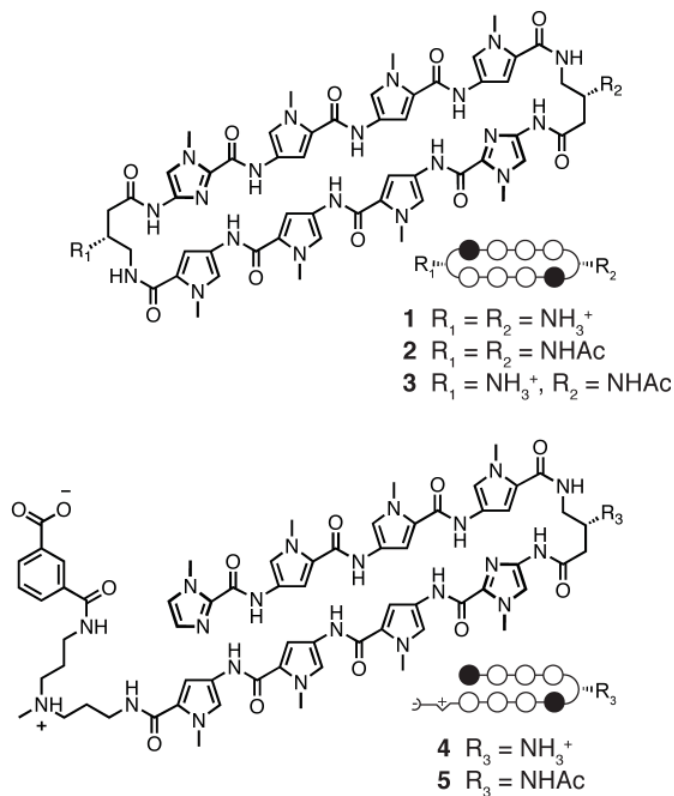
Figure 3.1 Structures of cyclic and hairpin polyamides **1–5** targeted to the DNA sequence 5'-WGWWCW-3' and their ball-and-stick models. Ball-and-stick representation legend: black and white circles represent *N*-methylimidazole and *N*-methylpyrrole units, respectively, half-circle with - sign represents the terminal isophthalic acid substituent, and white half-diamond with + sign represents the triamine linker unit.

solid-phase protocols are characterized by low reaction yields due to inefficient macrocyclization.[10] We report here the solution-phase synthesis of cyclic polyamides **1–3** with an improved high–yield cyclization step. In addition, we examined the DNA binding properties of these compounds by thermal duplex DNA melting and performed preliminary studies of their *in vitro* ADMET properties. Cyclic Py-Im polyamides **1–3** were shown to regulate endogenous gene expression in cell culture experiments.

3.2 Results and Discussion

3.2.1 Solution-Phase Synthesis of Cyclic Polyamides

Due to the symmetrical nature of cyclic polyamides **1–3** and their sequence similarity to previously described hairpin polyamide **4**,[11] PyPyPy trimer **6** and Im-turn dimer **7** provide all the necessary atoms to synthesize **1–3**. The preparation of advanced intermediates **6** and **7** has been detailed in the Chapter 2 (this thesis)[11] from readily available building blocks.[12] The cornerstone of our synthesis strategy capitalizes on the disparate physical properties of starting materials versus products, which permit purification of most intermediates to be achieved by combinations of precipitation, trituration, and crystallization. In addition, *in situ* deprotection of advanced pentafluorophenyl ester polyamide **14** at high dilution leads to macrocyclization in high yield, affording cyclic polyamide **15**.

The synthesis of tetramer-turn **9** begins with Im-turn dimer **7** (Scheme 3.1). Saponification of **7** with aqueous KOH in methanol at 37 °C, followed by neutralization, precipitation, and Et$_2$O trituration, yields Im-turn acid **8** in 95% yield. Amide coupling of **8** with pyrrole trimer **6** provides pentamer **9** in 96% yield. The utilization of a small excess of **6** relative to **8** drives the reaction to completion, and residual **6** is readily separated from **9** following precipitation in water and aqueous washing of residual solid
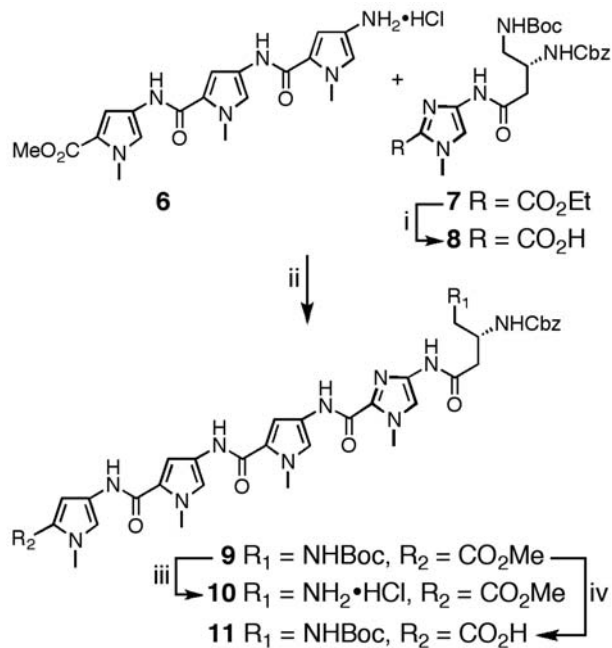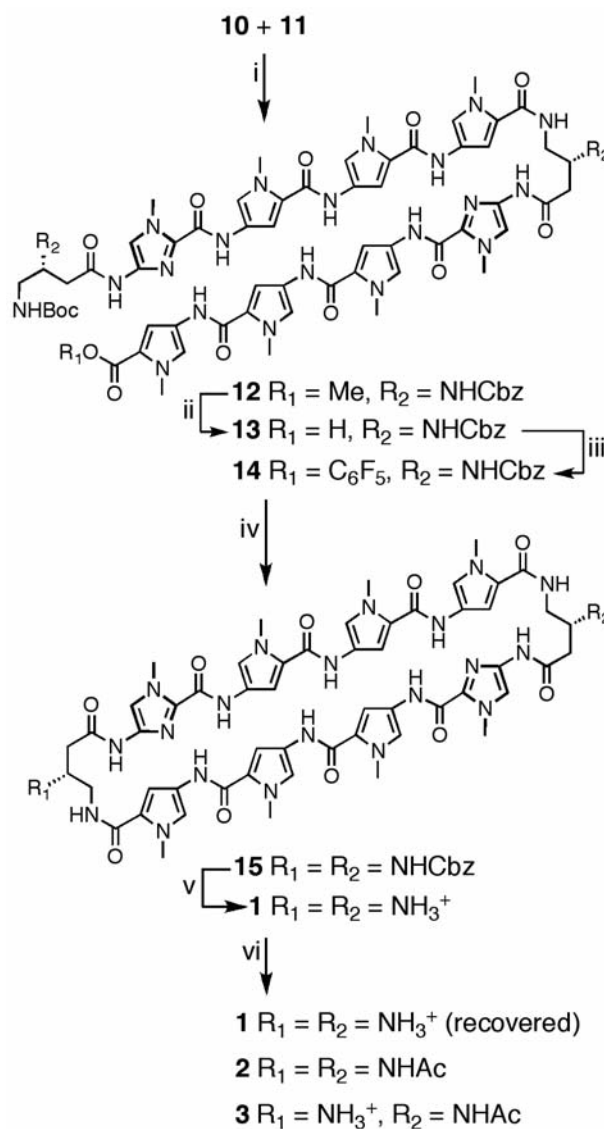
Scheme 3.1 Preparation of **10** and **11**. Reagents and Conditions: (i) KOH (aq), MeOH, 37 °C, 2 h, 95%; (ii) **8**, PyBOP, DMF, DIEA, **6**, 23 °C, 4 h, 96%; (iii) HCl in 1,4-dioxane, 23 °C, 2 h, 99% (iv) NaOH (aq), 1,4-dioxane, 42 °C, 3 h, 95%.

9. With all atoms in place for the target cyclic polyamide **1**, compound **9** was elaborated to amine salt **10** (99% yield) by reaction with HCl in 1,4-dioxane. Carboxylic acid **11** was generated by saponification of **9** with NaOH in 1,4-dioxane in 95% yield.

Assembly of the acyclic advanced intermediate **12** was achieved by PyBOP-mediated coupling of intermediates **10** and **11** in 94% yield (Scheme 3.2). A small excess of amine salt **10** was utilized to drive the reaction to completion. Saponification of ester **12** proceeded smoothly with aqueous NaOH in 1,4-dioxane, yielding **13** in 93% yield. Activation of acid **13** as the pentafluorophenol ester **14** provided the necessary functionality to afford macrocyclization following removal of the terminal *tert*-butyl carbamate (Boc) protecting group. In our hands, we found that the pentafluorophenol ester sufficiently activated the terminal acid for amide coupling while avoiding undesired oligomerization and/or decomposition processes that are conceivable with more reactive functionalities, such as acid chlorides. Premature initiation of the macrocyclization reaction was tempered by keeping the terminal amine protonated until it was

Scheme 3.2 Preparation of **1**, **2**, and **3**. Reagents and Conditions: (i) PyBOP, DMF, DIEA, 23 °C, 2 h, 94%; (ii) NaOH (aq), 1,4-dioxane, 40 °C, 4 h, 93%; (iii) CH_2Cl_2, DCC, pentafluorophenol, DMAP, 23 °C, 12 h, 80%; (iv) a) CF_3CO_2H, CH_2Cl_2, 23 °C, concentrate; b) DMF, acetonitrile, DIEA, 0–23 °C, 3 days; (v) CF_3SO_3H, CF_3CO_2H, 23 °C, 5 min, 68% over 3 steps; (vi) NMP, DIEA, Ac_2O, 23 °C, 18% of **1** (recovered), 22% of **2**, 40% of **3**.

transferred into a dilute solution of acetonitrile. Addition of an amine base (DIEA) then generated the free terminal amine, which could then undergo macrocyclization in dilute solvent conditions to deliver **15**, which was directly deprotected following purification. The benzyl carbamate protecting

groups were cleaved by treatment with superacid conditions (trifluoromethylsulfonic acid–trifluoroacetic acid) to provide **1** in 68% yield over three steps. Controlled acetylation of **1** by reaction with substoichiometric quantities of Ac$_2$O in NMP/DIEA provided a statistical population of **1** (18%), **2** (22%), and **3** (40%) that were easily separable by preparative HPLC. Acetylated hairpin **5** was prepared using excess Ac$_2$O/pyridine in 95% yield from previously reported amine hairpin **4**.[11]

Table 3.1 T_m values for polyamides for **1–5**.[a]

ARE dsDNA sequence =	5'-TTGC **TGTTCT** GCAA-3' 3'-AACG **ACAAGA** CGTT-5'	
Polyamides	T_m / °C	ΔT_m / °C
—	60.0 (±0.3)	—
(1)	83.5 (±0.5)	23.6 (±0.6)
(2)	81.2 (±0.2)	21.3 (±0.4)
(3)	82.0 (±0.0)	22.1 (±0.3)
(4)	78.4 (±0.5)	18.4 (±0.6)
(5)	76.0 (±0.5)	16.1 (±0.6)

[a]All values reported are derived from at least three melting temperature experiments with standard deviations indicated in parentheses. ΔTm values are given as $Tm^{(DNA/polyamide)} - Tm^{(DNA)}$. The propagated error in ΔTm measurements is the square root of the sum of the square of the standard deviations for the Tm values.

3.2.2 Thermal Stabilization of DNA duplexes by Polyamides
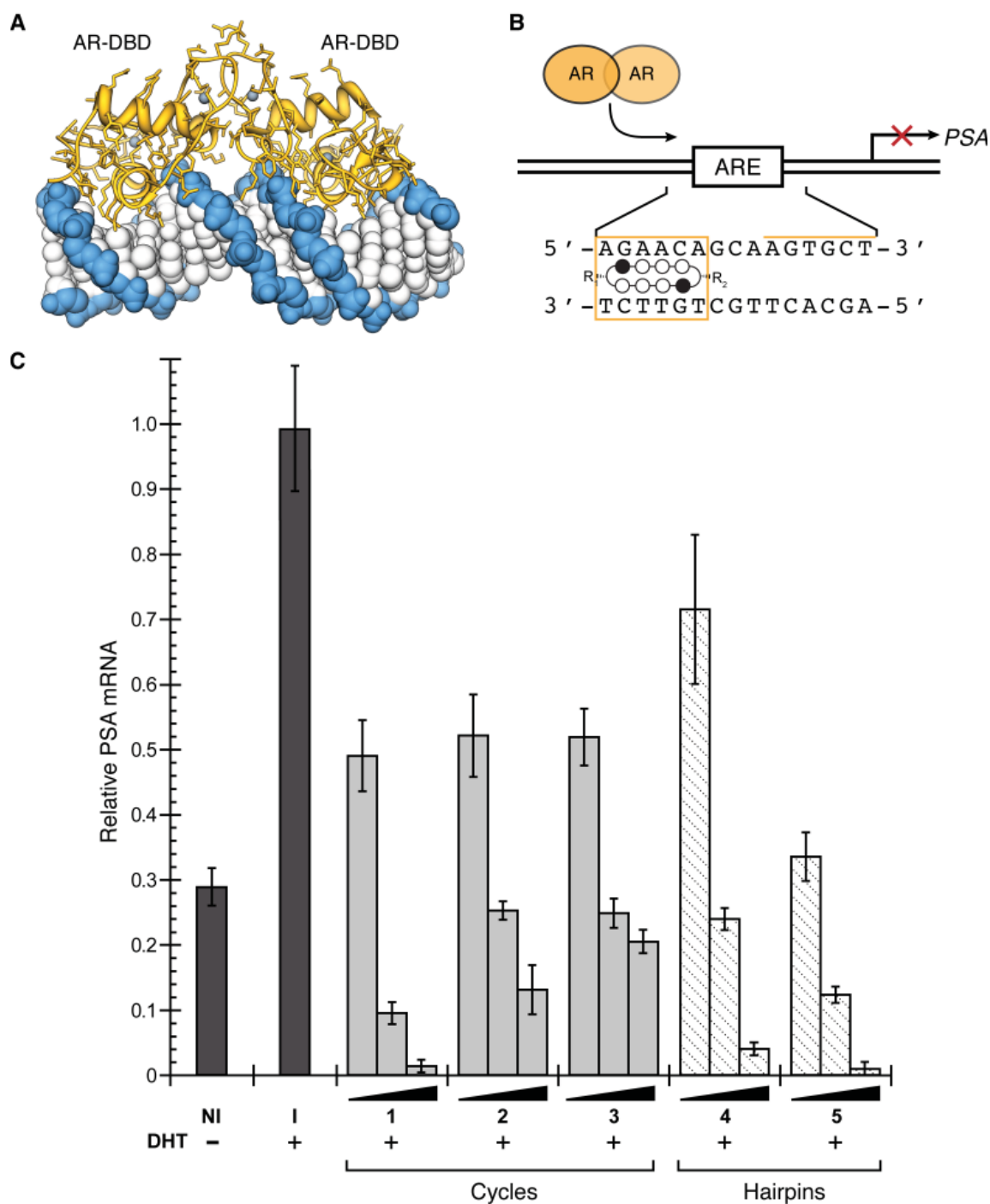
Quantitative DNase I footprint titrations have historically been utilized to measure polyamide–DNA binding affinities and specificities.[13] However, this method is limited to measuring K_a values $\leq 2 \times 10^{10}$ M^{-1}, which invalidates this technique for quantifying the exceptionally high DNA-binding affinities of cycles **1–3**.[14] The magnitude of DNA thermal stabilization (ΔT_m) of DNA–polyamide complexes has been utilized to rank order polyamides with high DNA binding affinities.[5g,15] Accordingly, we have employed melting temperature analysis (ΔT_m) for dissecting differences in DNA-binding affinities of hairpin versus cyclic polyamides. Spectroscopic analyses were performed on a 14-mer duplex DNA mimicking the androgen response element (ARE) DNA sequence, 5′-TTGCTGTTCTGCAA-3′ DNA duplex, which contains one polyamide binding site. As shown in Table 3.1 polyamides **1–5** provided an increase in the duplex DNA melting temperature relative to the individual DNA duplex, thereby confirming polyamide-DNA binding. Chiral hairpin **4** led to an increased melting temperature ΔT_m = 18.4 °C whereas cyclic polyamide **1** yielded a higher ΔT_m-value of 23.6 °C. Cyclic polyamides **1–3** reveal stronger stabilizations than parent hairpin analogs **4** and **5**. Acylation of the β-amino turns was shown to decrease the thermal stabilization values in both hairpin and cyclic motifs, presumably due to the loss of beneficial electrostatics from the protonated-cationic amine on the turn unit.

A AR-DBD AR-DBD

B AR AR

PSA

ARE

5'-AGAACAGCAAGTGCT-3'

R_1 R_2

3'-TCTTGTCGTTCACGA-5'

C

Relative PSA mRNA

1.0
0.9
0.8
0.7
0.6
0.5
0.4
0.3
0.2
0.1
0

NI I 1 2 3 4 5
DHT − + + + + + +

Cycles   Hairpins

Figure 3.2 Targeting the ARE with DNA-binding polyamides. (a) X-ray crystal structure of androgen receptor homodimer DNA-binding domain bound to the sequence 5'-CTGTTCTTGATGT-TCTGG-3' (PDB 1r4i).[16] (b) Map of the PSA-ARE site (top) and schematic representation of a cyclic polyamide targeting the PSA-ARE site 5'-AGAACA-3'. (c) Inhibition of induced PSA mRNA expression in LNCaP cells by cyclic PI polyamides **1–3** and hairpin polyamides **4** and **5** (dosed at 0.3, 3, and 30 µM) by real-time quantitative PCR. The results were normalized to a DHT-induced, untreated control (control=1), and the error bars represent the standard error of the mean of a single experiment performed in biological triplicate. The entire experiment was reproduced four times, with similar results. NI = noninduced, I = induced, DHT = dihydrotestosterone.

3.2.3 Biological Assay for Cell Permeability

Hairpin polyamides have been shown to modulate endogenous gene expression in living cells by disrupting transcription factor–DNA binding in gene promoters.[2,7-9] Recently, hairpin polyamide **4** was shown to inhibit androgen receptor-mediated expression of prostate-specific antigen (PSA) in LNCaP cells by targeting the DNA sequence 5´-AGAACA-3´ found in the ARE.[5g] We utilized this cell culture transcription assay to investigate the biological activity of cyclic polyamides **1–3** in comparison to hairpin polyamides **4** and **5**. Since small structural changes to polyamides have been shown to correlate with differences in cellular uptake properties,[5] it was not obvious whether cyclic polyamides **1–3** would permeate cell membranes and exhibit biological activity comparable to that of hairpin polyamides **4** and **5**. Quantitative real-time RT-PCR analysis of DHT-induced PSA expression revealed that cyclic polyamides **1–3** all decreased PSA mRNA levels in LNCaP cells, with cycle **1** exhibiting activity comparable to that of acetylated hairpin polyamide **5** (Figure 3.2). On the basis of these results, we can infer that this class of cyclic Py-Im polyamides are cell permeable and can regulate endogenous gene expression in cell culture.

*3.2.4 ADMET Studies of Polyamides **1** and **5***

Due to the promising cell culture results obtained with cyclic polyamide **1** and hairpin polyamide **5** against PSA gene expression, we contracted preclinical *in vitro* absorption, distribution, metabolism, excretion, and toxicity (ADMET)[17] studies for both compounds.[18] Results from this study are summarized below and additional detail can be found in section 3.6 (Spectra and Supporting Information) and Appendix B of this thesis. Polyamides **1** and **5** were both found to exhibit low Caco-2 permeability, suggesting that neither compound may be orally available. Both **1** and **5** were found to be almost exclusively protein bound in plasma, with half-lives greater than 2 h. A recent positron emission tomography (PET)-based biodistribution study of a related hairpin polyamide in mice revealed high levels of liver occupancy following tail vein dosage.[19] On the basis of this result, we investigated the liver stability of candidate polyamides **1** and **5**. Microsomal intrinsic clearance studies found half-lives greater than 3 h for **1** and **5** in both human and rat liver microsomes, and no significant inhibition was measured against any cytochrome P450 isoform examined (Cyp1A2/CEC, Cyp2C8/DBF, Cyp2C9/DBF, Cyp2C19/DBF, Cyp2D6/AMMC, Cyp3A4/BFC, Cyp3A4/DBF). Furthermore, no obvious toxicity ($IC_{50} > 100$ μM) was observed in the human hepatocellular carcinoma cell line HepG2. In addition, standard hERG FastPatch assays of cardiac toxicity found that both polyamides (**1** and **5**) were devoid of unwanted inhibition (IC_{50}

> 100 μM).

3.3 Conclusion

We describe a solution-phase synthesis methodology for preparing cyclic Py-Im polyamides, highlighted by an efficient macrocyclization between the alkyl linker amine and a pentafluorophenol ester-activated amino acid. The three cyclic Py-Im polyamides possessed high DNA-binding affinities and were capable of accessing the nucleus in cell culture, as judged by their ability to downregulate AR-activated PSA expression in cell culture. Preclinical ADMET analysis of cyclic polyamide **1** and hairpin polyamide **5** revealed favorable drug-like properties such as high liver stability and low toxicity. Ongoing work is focused on characterizing the precise molecular interactions between cyclic polyamides and their cognate DNA sequences by high-resolution crystallographic studies.

3.4 Experimental Section

3.4.1 General

Chemicals and solvents were purchased from Sigma-Aldrich and were used without further purification. (*R*)-3,4-Cbz-Dbu(Boc)-OH was purchased from Senn Chemicals AG (code number 44159). All DNA oligomers were purchased HPLC purified from Integrated DNA Technologies. Water (18 MΩ) was purified using a Millipore Milli-Q purification system. Centrifugation was performed in a Beckman Coulter benchtop centrifuge (Allegra 21R) equipped with a Beckman swing-out rotor (model S4180). Analytical HPLC analysis was conducted on a Beckman Gold instrument equipped with a Phenomenex Gemini analytical column (250 × 4.6 mm, 5 μm) and a diode array detector, and the mobile phase consisted of a gradient of acetonitrile (MeCN) in 0.1% (v/v) aqueous CF_3CO_2H. Preparative HPLC was performed on an Agilent 1200 system equipped with a solvent degasser, a diode array detector, and a Phenomenex Gemini column (250 × 21.2 mm, 5 μm). A gradient of MeCN in 0.1% (v/v) aqueous CF_3CO_2H was utilized as the mobile phase. UV–Vis measurements were made on a Hewlett-Packard diode array spectrophotometer (model 8452 A), and polyamide concentrations were measured in 0.1% (v/v) aqueous CF_3CO_2H using an extinction coefficient of 69200 $M^{-1} \cdot cm^{-1}$ at λ_{max} near 310 nm. NMR spectroscopy was performed on a Varian instrument operating at 499.8 (for ^1H) or 125.7 MHz (for ^{13}C) at ambient temperature. All NMR analyses were performed in DMSO-d_6, and chemical shifts are reported in parts per million relative to the internal solvent peak referenced to 2.49 (for ^1H) or 39.5 (for ^{13}C). High-resolution

mass spectrometry (HRMS) was recorded in positive-ion mode by fast-atom bombardment (FAB⁺) on a JEOL JMS-600H instrument or by electrospray ionization (ESI⁺) on a Waters Acquity UPLC-LCT Premiere XE TOF-MS system.

3.4.2 UV Absorption Spectrophotometry

Melting temperature analysis was performed on a Varian Cary 100 spectrophotometer equipped with a thermo-controlled cell holder possessing a cell path length of 1 cm. A degassed aqueous solution of 10 mM sodium cacodylate, 10 mM KCl, 10 mM $MgCl_2$, and 5 mM $CaCl_2$ at pH 7.0 was used as analysis buffer. DNA duplexes and polyamides were mixed in 1:1 stoichiometry to a final concentration of 2 μM for each experiment. Prior to analysis, samples were heated to 90 °C and cooled to a starting temperature of 23 °C with a heating rate of 5 °C/min for each ramp. Denaturation profiles were recorded at $\lambda = 260$ nm from 23 to 90 °C with a heating rate of 0.5 °C/min. The reported melting temperatures were defined as the maximum of the first derivative of the denaturation profile.

3.4.3 Measurement of Androgen-Induced PSA mRNA

Experiments were performed as described previously[8] with the following modifications: (1) all compounds and controls were prepared in neat DMSO and then diluted with media to a final concentration of 0.1% DMSO, and (2) mRNA was isolated with the RNEasy 96 kit (Qiagen, Valencia, CA).

3.4.4 BocHN-(R)^{β-CbzHN}γ-Im-CO₂H (8)

A solution of BocHN-(R)^{β-CbzHN}γ-Im-CO₂Et **7** (450 mg, 0.894 mmol) dissolved in MeOH (1.0 mL) and aqueous KOH (1 N, 2.0 mL, 2.0 mmol) was stirred at 37 ºC for 2 h. The reaction mixture was added to a cooled (ice bath) solution of distilled H_2O (10 mL) preacidified with aqueous HCl (1 N, 2.0 mL, 2.0 mmol), yielding a precipitate that was isolated by centrifugation (~4500 rpm). The residual solid was again suspended in distilled H_2O (10 mL) and collected by centrifugation. The resultant solid, which contained a small amount of residual H_2O, was frozen and lyophilized to dryness and then suspended in excess anhydrous Et_2O and filtered, and the filter cake washed with copious amounts of anhydrous Et_2O. Drying of the brown solid *in vacuo* yielded saponified dimer **8** (404 mg, 95%). ¹H NMR: δ 10.46 (s, 1H), 7.47 (s, 1H), 7.31-7.26 (m, 5H), 7.02 (d, $J = 8.3$ Hz, 1H), 6.79 (t, $J = 5.4$ Hz, 1H), 4.97 (s, 2H), 3.92 (m, 1H), 3.88 (s, 3H), 3.60 (s, 1H), 3.01 (m, 2H),

2.41 (m, 2H), 1.35 (s, 9H); ^{13}C NMR: δ 167.6, 160.0, 155.8, 155.4, 137.11, 137.09, 131.6, 128.2, 127.66, 127.55, 114.6, 77.7, 65.1, 48.7, 43.5, 38.0, 35.4, 28.2; HRMS (FAB$^+$) calc'd for C$_{22}$H$_{30}$N$_5$O$_7$ [M+H]$^+$ 476.2145, found 476.2130.

3.4.5 BocHN-(R)$^{β\text{-}CbzHN}$γ-ImPyPyPy-CO$_2$Me (9)

A solution of BocHN-(*R*)$^{β\text{-}CbzHN}$γ-Im-CO$_2$H **8** (300 mg, 0.631 mmol) and PyBOP (345 mg, 0.663 mmol) in DMF (3.2 mL) and DIEA (330 μL, 1.9 mmol) was stirred at 23 °C for 10 min. The solution was then treated with solid (powdered) HCl•H$_2$N-PyPyPy-CO$_2$Me **6** (288 mg, 0.663 mmol) and stirred at 23 °C for 4 h. The solution was then added to distilled H$_2$O (10 mL) preacidified with aqueous HCl (1 N, 2 mL, 2 mmol), yielding a precipitate that was isolated by centrifugation (~4500 rpm). The residual solid was again suspended in distilled H$_2$O (10 mL) and collected by centrifugation (repeated 3x). The resultant solid, which contained a small amount of residual H$_2$O, was frozen and lyophilized to dryness. The solid was triturated with anhydrous Et$_2$O and filtered over a sintered glass funnel. The resultant solid was washed with copious amounts of anhydrous Et$_2$O and dried *in vacuo* to yield BocHN-(*R*)$^{β\text{-}CbzHN}$γ-ImPyPyPy-CO$_2$Me **9** as a tan solid (518 mg, 96%). ^{1}H NMR: δ 10.17 (s, 1H), 10.00 (s, 1H), 9.95 (s, 1H), 9.93 (s, 1H), 7.46 (d, *J* = 1.7 Hz, 1H), 7.44 (s, 1H), 7.31-7.29 (m, 5H), 7.27 (d, *J* = 1.7 Hz, 1H), 7.23 (d, *J* = 1.7 Hz, 1H), 7.14 (d, *J* = 1.7 Hz, 1H), 7.07 (d, *J* = 1.7 Hz, 1H), 7.04 (d, *J* = 8.3 Hz, 1H), 6.90 (d, *J* = 2.0 Hz, 1H), 6.81 (t, *J* = 5.9 Hz, 1H), 4.98 (s, 2H), 3.96 (m, 1H), 3.95 (s, 3H), 3.85 (s, 3H), 3.84 (s, 3H), 3.83 (s, 3H), 3.73 (s, 3H), 3.03 (m, 2H), 2.46 (m, 2H), 1.36 (s, 9H); ^{13}C NMR: δ 167.8, 160.8, 158.5, 158.4, 155.84, 155.81, 155.5, 137.1, 136.0, 134.0, 128.3, 127.7, 127.6, 123.06, 123.00, 122.5, 122.2, 121.2, 120.7, 118.7, 118.6, 118.5, 114.0, 108.4, 104.9, 77.8, 65.2, 50.9, 48.8, 43.6, 38.2, 36.20, 36.18, 36.09, 34.9, 28.2; HRMS (FAB$^+$) calc'd for C$_{41}$H$_{49}$N$_{11}$O$_{10}$ [M$^•$]$^+$ 855.3663, found 855.3688.

3.4.6 HCl•H2N-(R)$^{β\text{-}CbzHN}$γ-ImPyPyPy-CO$_2$Me (10)

A solution of BocHN-(R)$^{β\text{-}CbzHN}$γ-ImPyPyPy-CO$_2$Me **9** (125 g, 0.146 mmol) in anhydrous HCl in 1,4-dioxane (4.0 M, 10 mL) was stirred at 23 °C for 2 h. The mixture was then diluted with 100 mL of anhydrous Et$_2$O and filtered over a sintered glass funnel. The resultant solid was washed with copious amounts of anhydrous Et$_2$O and dried in vacuo to yield HCl•H$_2$N-(R)$^{β\text{-}CbzHN}$γ-ImPyPyPy-CO$_2$Me **10** as a brown solid (114 mg, 99%). ^{1}H NMR: δ 10.38 (s, 1H), 9.98 (s, 1H), 9.96 (s, 1H), 9.94 (s, 1H), 8.10 (m, 3H), 7.46 (d, *J* = 1.7 Hz, 1H), 7.45 (s, 1H), 7.42 (d, *J* = 8.3 Hz, 1H), 7.34-7.28 (m, 5H), 7.28 (d, *J* = 1.7 Hz, 1H), 7.24 (d, *J* = 1.7 Hz, 1H), 7.16 (d, *J* = 1.7 Hz, 1H), 7.08 (d, *J* = 1.7

Hz, 1H), 6.90 (d, J = 1.7 Hz, 1H), 5.02 (m, 2H), 4.14 (m, 1H), 3.95 (s, 3H), 3.85 (s, 3H), 3.84 (s, 3H), 3.83 (s, 3H), 3.73 (s, 3H), 3.02 (m, 2H), 2.63 (m, 2H); ^{13}C NMR: δ 167.0, 160.8, 158.5, 158.4, 155.7, 136.8, 135.7, 134.0, 128.3, 127.8, 127.7, 123.05, 122.97, 122.5, 122.2, 121.1, 120.7, 118.64, 118.60, 118.5, 108.4, 104.9, 65.6, 50.9, 46.7, 42.0, 38.2, 36.2, 36.1, 36.0, 34.9; HRMS (FAB$^+$) calc'd for $C_{36}H_{42}N_{11}O_8$ [M+H]$^+$ 756.3218, found 756.3211.

3.4.7 BocHN-(R)$^{β\text{-}CbzHN}$γ-ImPyPyPy-CO$_2$H (11)

A solution of BocHN-(R)$^{β\text{-}CbzHN}$γ-ImPyPyPy-CO$_2$Me **9** (200 mg, 0.234 mmol) dissolved in 1,4-dioxane (2.3 mL) and aqueous NaOH (1 N, 2.3 mL, 2.3 mmol) was stirred at 42 ºC for 3 h. The solution was then added to distilled H$_2$O (5 mL) preacidified with aqueous HCl (1 N, 2.3 mL, 2.3 mmol), yielding a precipitate that was isolated by centrifugation (~4500 rpm). The residual solid was again suspended in distilled H$_2$O (10 mL) and collected by centrifugation (repeated 2x). The resultant solid, which contained a small amount of residual H$_2$O, was frozen and lyophilized to dryness and then suspended in excess anhydrous Et$_2$O and filtered, and the filter cake washed with copious amounts of anhydrous Et$_2$O. Drying of the tan solid *in vacuo* yielded BocHN-(R)$^{β\text{-}CbzHN}$γ-ImPyPyPy-CO$_2$H **11** (187 mg, 95%). ^{1}H NMR: δ 12.15 (s, 1H), 10.21 (s, 1H), 10.00 (s, 1H), 9.96 (s, 1H), 9.92 (s, 1H), 7.44 (s, 1H), 7.42 (d, J = 1.7 Hz, 1H), 7.31-7.29 (m, 5H), 7.28 (d, J = 1.5 Hz, 1H), 7.24 (d, J = 1.5 Hz, 1H), 7.16 (d, J = 1.5 Hz, 1H), 7.08 (m, 2H), 6.85 (d, J = 1.7 Hz, 1H), 6.82 (t, J = 5.7 Hz, 1H), 4.98 (s, 2H), 3.95 (m, 4H), 3.85 (s, 3H), 3.84 (s, 3H), 3.81 (s, 3H), 3.03 (m, 2H), 2.46 (m, 2H), 1.36 (s, 9H); ^{13}C NMR: δ 167.8, 162.0, 158.44, 158.38, 155.80, 155.77, 155.4, 137.1, 136.0, 133.9, 128.3, 127.7, 127.6, 123.0, 122.7, 122.6, 122.2, 121.2, 120.2, 119.5, 118.6, 118.5, 114.0, 108.4, 104.87, 104.83, 77.7, 65.1, 48.8, 43.5, 38.2, 36.2, 36.13, 36.06, 34.9, 28.2; HRMS (FAB$^+$) calc'd for $C_{40}H_{47}N_{11}O_{10}$ [M$^{•}$]$^+$ 841.3507, found 841.3498.

3.4.8 BocHN-(R)$^{β\text{-}CbzHN}$γ-ImPyPyPy-(R)$^{β\text{-}CbzHN}$γ-ImPyPyPy-CO$_2$Me (12)

A solution of BocHN-(R)$^{β\text{-}CbzHN}$γ-ImPyPyPy-CO$_2$H **11** (25 mg, 0.029 mmol) and PyBOP (17 mg, 0.031 mmol) in DMF (150 μL) and DIEA (16 μL, 0.089 mmol) was stirred at 23 ºC for 20 min. The solution was then treated with solid (powdered) HCl•H$_2$N-(R)$^{β\text{-}CbzHN}$γ-ImPyPyPy-CO$_2$Me **10** (25 mg, 0.031 mmol) and stirred at 23 ºC for 2 h. The solution was then added to distilled H$_2$O (10 mL) preacidified with aqueous HCl (1 N, 1 mL, 1 mmol), yielding a precipitate that was isolated by centrifugation (~4500 rpm). The residual solid was again suspended in distilled H$_2$O (10 mL) and collected by centrifugation (repeated 3x). The resultant solid, which contained a small amount of

residual H$_2$O, was frozen and lyophilized to dryness. The solid was triturated with anhydrous Et$_2$O and filtered over a sintered glass funnel. The resultant solid was washed with copious amounts of anhydrous Et$_2$O and dried *in vacuo* to yield BocHN-(*R*)$^{\beta\text{-CbzHN}}\gamma$-ImPyPyPy-(*R*)$^{\beta\text{-CbzHN}}\gamma$-ImPyPyPy-CO$_2$Me **12** as a tan solid (44 mg, 94%). ^{1}H NMR: δ 10.20 (s, 1H), 10.16 (s, 1H), 9.98 (s, 2H), 9.94-9.91 (m, 4H), 7.99 (m, 1H), 7.46 (d, *J* = 1.7 Hz, 1H), 7.45 (s, 1H), 7.44 (s, 1H), 7.32-7.14 (m, 18H), 7.07 (m, 2H), 7.03 (d, *J* = 8.3 Hz, 1H), 6.92 (s, 1H), 6.90 (d, *J* = 2.0 Hz, 1H), 6.80 (t, *J* = 5.6 Hz, 1H), 4.99 (m, 4H), 4.10 (m, 1H), 3.95 (m, 7H), 3.85-3.83 (m, 15H), 3.79 (s, 3H), 3.73 (s, 3H), ~3.30 (m, 2H, obstructed by H$_2$O peak), 3.04 (m, 2H), 2.53-2.44 (m, 4H, partially obstructed by NMR solvent), 1.36 (s, 9H); ^{13}C NMR: δ 167.9, 167.8, 161.6, 160.8, 158.5, 158.44, 158.42, 155.8, 155.6, 155.5, 137.1, 136.0, 134.00, 133.98, 128.3, 127.7, 127.63, 127.60, 123.11, 123.07, 123.00, 122.80, 122.77, 122.5, 122.3, 122.2, 122.1, 121.3, 120.8, 118.69, 118.66, 118.62, 118.52, 118.0, 114.1, 108.4, 104.9, 104.8, 104.5, 77.8, 65.21, 65.16, 50.9, 48.83, 48.78, 43.6, 42.2, 38.4, 38.2, 36.2, 36.10, 36.07, 36.0, 34.9, 28.2; HRMS (TOF-ESI$^+$) calc'd for C$_{76}$H$_{87}$N$_{22}$O$_{17}$ [M+H]$^+$ 1579.6620, found 1579.6580.

3.4.9 BocHN-(*R*)$^{\beta\text{-CbzHN}}\gamma$-ImPyPyPy-(*R*)$^{\beta\text{-CbzHN}}\gamma$-ImPyPyPy-CO$_2$H (*13*)

A solution of BocHN-(*R*)$^{\beta\text{-CbzHN}}\gamma$-ImPyPyPy-(*R*)$^{\beta\text{-CbzHN}}\gamma$-ImPyPyPy-CO$_2$Me **12** (25 mg, 0.0158 mmol) dissolved in 1,4-dioxane (376 μL) and aqueous NaOH (1 N, 253 μL, 0.253 mmol) was stirred at 40 ℃ for 4 h. The solution was then added to distilled H$_2$O (5 mL) preacidified with aqueous HCl (1 N, 253 μL, 0.253 mmol), yielding a precipitate that was diluted with another 15 mL of H$_2$O and was then isolated by centrifugation (~4500 rpm). The resultant solid, which contained a small amount of residual H$_2$O, was frozen and lyophilized to dryness and then suspended in excess anhydrous Et$_2$O, triturated, and filtered, and the filter cake washed with copious amounts of anhydrous Et$_2$O. Drying of the tan solid *in vacuo* yielded BocHN-(*R*)$^{\beta\text{-CbzHN}}\gamma$-ImPyPyPy-(*R*)$^{\beta\text{-CbzHN}}\gamma$-ImPyPyPy-CO$_2$H **13** (23 mg, 93%). ^{1}H NMR: δ 12.13 (br s, 1H), 10.23 (s, 1H), 10.20 (s, 1H), 9.98-9.90 (m, 6H), 8.01 (m, 1H), 7.443 (s, 1H), 7.439 (s, 1H), 7.42 (d, *J* = 1.7 Hz, 1H), 7.30-7.15 (m, 18H), 7.07 (m, 3H), 6.92 (m, 1H), 6.84 (d, *J* = 2.0 Hz, 1H), 6.81 (t, *J* = 5.6 Hz, 1H), 5.00 (m, 2H), 4.98 (s, 2H), 4.10 (m, 1H), 3.95 (m, 7H), 3.85-3.83 (m, 12H), 3.81 (s, 3H), 3.78 (s, 3H), ~3.30 (m, 2H, obstructed by H$_2$O peak), 3.03 (m, 2H), 2.53 (m, 2H), 2.46 (m, 2H), 1.36 (s, 9H); ^{13}C NMR: δ 167.94, 167.87, 162.4, 162.0, 161.6, 158.54, 158.50, 158.43, 155.8, 155.75, 155.74, 155.6, 155.5, 137.1, 136.0, 133.91, 133.90, 128.3, 127.7, 127.60, 127.57, 123.10, 123.07, 122.8, 122.7, 122.6, 122.3, 122.24, 122.17, 121.16, 121.15, 120.3, 119.5, 118.64, 118.61, 118.5, 118.0, 114.10,

114.06, 108.5, 105.0, 104.5, 77.8, 65.2, 65.1, 48.8, 43.6, 42.2, 38.4, 38.2, 36.2, 36.14, 36.10, 36.08, 36.0, 35.8, 34.9, 28.2; HRMS (TOF-ESI$^+$) calc'd for $C_{75}H_{86}N_{22}O_{17}$ [M+2H]$^{2+}$/2 783.3271, found 783.3237.

3.4.10 BocHN-(R)$^{β-CbzHN}$γ-ImPyPyPy-(R)$^{β-CbzHN}$γ-ImPyPyPy-CO$_2$Pfp (14)

A solution of BocHN-(R)$^{β-CbzHN}$γ-ImPyPyPy-(R)$^{β-CbzHN}$γ-ImPyPyPy-CO$_2$H **13** (250 mg, 0.160 mmol) and DCC (66 mg, 0.320 mmol) in CH_2Cl_2 (8.8 mL) was stirred at 23 ºC for 45 min. The solution was then treated with DMAP (2 mg, 0.016 mmol) followed by pentafluorophenol (175 mg, 0.950 mmol) and stirred at 23 ºC for 12 h. The reaction mixture was then loaded onto a silica gel column with CH_2Cl_2 and eluted with step gradients of 100% CH_2Cl_2 to 100% acetone with incremental steps of 5% acetone. The product was concentrated *in vacuo* to yield BocHN-(R)$^{β-CbzHN}$γ-ImPyPyPy-(R)$^{β-CbzHN}$γ-ImPyPyPy-CO$_2$Pfp **14** as a brown solid (221 mg, 80%). ^{1}H NMR: δ 10.20 (s, 1H), 10.16 (s, 1H), 10.08 (s, 1H), 9.99-9.91 (m, 5H), 7.99 (m, 1H), 7.73 (d, J = 1.7 Hz, 1H), 7.444 (s, 1H), 7.440 (s, 1H), 7.30-7.12 (m, 20 H), 7.06 (d, J = 1.2 Hz, 1H), 7.03 (d, J = 8.5 Hz, 1H), 6.92 (s, 1H), 6.80 (t, J = 5.4 Hz, 1H), 5.00 (m, 2H), 4.98 (m, 2H), 4.11 (m, 1H), 3.95 (m, 7H), 3.88 (s, 3H), 3.86-3.84 (m, 12H), 3.78 (s, 3H), ~3.30 (m, 2H, obstructed by H$_2$O peak), 3.04 (m, 2H), 2.52 (m, 2H), 2.46 (m, 2H), 1.36 (s, 9H); HRMS (TOF-ESI$^+$) calc'd for $C_{81}H_{85}F_5N_{22}O_{17}$ [M+2H]$^{2+}$/2 866.3192, found 866.3236.

3.4.11 cyclo-(-ImPyPyPy-(R)$^{β-H2N}$γ-ImPyPyPy-(R)$^{β-H2N}$γ-) (1)

A solution of BocHN-(R)$^{β-CbzHN}$γ-ImPyPyPy-(R)$^{β-CbzHN}$γ-ImPyPyPy-CO$_2$Pfp **14** (84 mg, 0.049 mmol) in anhydrous CF_3CO_2H:CH_2Cl_2 (1:1, 4 mL) was stirred at 23 ºC for 10 min prior to being concentrated to dryness in a 500 mL round-bottom flask. The residue was then dissolved in cold (0 ºC) DMF (10 mL), followed by immediate dilution with MeCN (300 mL) and DIEA (1.6 mL). The reaction mixture was left at 23 ºC for 3 days without stirring. [Note: The solution turns cloudy as the macrocycliztion proceeds.] The reaction mixture was concentrated to a volume of 11 mL and added to a solution of H$_2$O (30 mL) and aqueous HCl (1 N, 9.2 mL) at 0 ºC. The protected intermediate cyclo-(-ImPyPyPy-(R)$^{β-CbzHN}$γ-ImPyPyPy-(R)$^{β-CbzHN}$γ-) **15** was isolated by centrifugation (~4500 rpm), lyophilized to dryness, and then suspended in excess anhydrous Et$_2$O, triturated, and filtered, and the filter cake washed with copious amounts of anhydrous Et$_2$O. Drying of the tan solid *in vacuo* yielded the protected intermediate cyclo-(-ImPyPyPy-(R)$^{β-CbzHN}$γ-ImPyPyPy-(R)$^{β-CbzHN}$γ-) **15**, HRMS (TOF-ESI$^+$) calc'd for $C_{70}H_{76}N_{22}O_{14}$ [M+2H]$^{2+}$/2 724.2956, found 724.2925. This material

was immediately deprotected by dissolving in CF_3CO_2H (2 mL) followed by addition of CF_3SO_3H (100 μL) at 23 ºC for 5 min. The solution was then frozen, and DMF (2 mL) was layered over the frozen solution. The thawed solution was diluted with H_2O (6 mL) and purified by reverse-phase HPLC to give a white solid after lyophilization. The solid was suspended in excess anhydrous Et_2O, triturated, filtered, and the filter cake washed with copious amounts of anhydrous Et_2O. Drying of the white solid *in vacuo* yielded cyclo-(-ImPyPyPy-(R)$^{\beta-H_2N}\gamma$-ImPyPyPy-(R)$^{\beta-H_2N}\gamma$-) **1** (46 mg, 68%). ^{1}H NMR: δ 10.56 (s, 2H), 9.91 (s, 4H), 9.88 (s, 2H), 8.17 (t, $J = 5.6$ Hz, 2H), 7.96 (m, 6H), 7.40 (s, 2H), 7.31 (d, $J = 1.6$ Hz, 2H), 7.27 (d, $J = 1.6$ Hz, 2H), 7.19 (d, $J = 1.6$ Hz, 2H), 7.00 (d, $J = 1.7$ Hz, 2H), 6.96 (d, $J = 1.6$ Hz, 2H), 6.94 (d, $J = 1.7$ Hz, 2H), 3.94 (s, 6H), 3.83 (s, 12H), 3.80 (s, 6H), 3.71 – 3.66 (m, 2H), 3.49 – 3.27 (m, 4H, partially obstructed by H_2O peak), 2.79 (dd, $J = 16.1$ Hz, 6.0 Hz, 2H), 2.60 (dd, $J = 15.2$ Hz, 5.2 Hz, 2H). HRMS (TOF-ESI$^+$) calc'd for $C_{54}H_{63}N_{22}O_{10}$ [M+H]$^+$ 1179.5098, found 1179.5087.

3.4.12 cyclo-(-ImPyPyPy-(R)$^{\beta-AcHN}\gamma$-ImPyPyPy-(R)$^{\beta-H2N}\gamma$-) (3) and cyclo-(-ImPyPyPy-(R)$^{\beta-AcHN}\gamma$-ImPyPyPy-(R)$^{\beta-AcHN}\gamma$-) (2)

A solution of cyclo-(-ImPyPyPy-(R)$^{\beta-H_2N}\gamma$-ImPyPyPy-(R)$^{\beta-H_2N}\gamma$-) **1** (2.81 mg, 2.0 μmol) in anhydrous NMP (200 μL) and DIEA (20 μL) at 23 ºC was treated with a solution of Ac_2O in NMP (0.122 M, 6.8 μL). After 10 min, the reaction mixture was treated with another 6.8 μL of Ac_2O in NMP (0.122 M) and allowed to stand for 5 h. The reaction mixture was then diluted to a volume of 10 mL by addition of a 4:1 solution of aqueous CF_3CO_2H (0.1% v/v):MeCN (5 mL), followed by additional aqueous CF_3CO_2H (0.1% v/v, 5 mL), and then purified by reverse-phase HPLC to yield cyclo-(-ImPyPyPy-(R)$^{\beta-H_2N}\gamma$-ImPyPyPy-(R)$^{\beta-H_2N}\gamma$-) **1** (363 nmol, 18%), cyclo-(-ImPyPyPy-(R)$^{\beta-AcHN}\gamma$-ImPyPyPy-(R)$^{\beta-H_2N}\gamma$-) **3** (800 nmol, 40%), and cyclo-(-ImPyPyPy-(R)$^{\beta-AcHN}\gamma$-ImPyPyPy-(R)$^{\beta-AcHN}\gamma$-) **2** (432 nmol, 22%). Cyclo-(-ImPyPyPy-(R)$^{\beta-AcHN}\gamma$-ImPyPyPy-(R)$^{\beta-H_2N}\gamma$-) **3** HRMS (TOF-ESI$^+$) calc'd for $C_{56}H_{65}N_{22}O_{11}$ [M+H]$^+$ 1221.5203, found 1221.5204. Cyclo-(-ImPyPyPy-(R)$^{\beta-AcHN}\gamma$-ImPyPyPy-(R)$^{\beta-AcHN}\gamma$-) **2** HRMS (TOF-ESI$^+$) calc'd for $C_{58}H_{68}N_{22}O_{12}$ [M+2H]$^{2+}$/2 633.2646, found 633.2631.

3.4.13 ImPyPyPy-(R)$^{\beta-H2N}\gamma$-ImPyPyPy-(+)-IPA (4)

Prepared as described in Chapter 2 of this thesis.[11]

3.4.14 ImPyPyPy-(R)$^{\beta-AcHN}\gamma$-ImPyPyPy-(+)-IPA (5)

A solution of polyamide **4**[11] (7.4 mg, 5.03 μmoles, assumes **4** as the mono-CF_3CO_2H salt) in DMF (1.76 mL) was treated with a solution of Ac_2O in pyridine (10% v/v, 240 μL, 0.254 mmoles Ac_2O). The solution was allowed to stand at 23 °C for 30 min, and then acidified with aqueous CF_3CO_2H (15% v/v, 2 mL). After 5 min the solution was further diluted with distilled H_2O (5 mL), purified by preparative RP-HPLC, and lyophilized to dryness. Suspension of the residual solid in anhydrous Et_2O, following by filtration and drying under high vacuum yielded **5** (6.7 mg, 95%). HRMS (FAB$^+$) calc'd for $C_{67}H_{79}N_{22}O_{13}$ [M+H]$^+$ 1399.6191, found 1399.6181.

3.5 Notes and References

1. Dervan, P. B. *Bioorg. Med. Chem.* **2001,** *9*, 2215–2235.

2. Dervan, P. B., and Edelson, B. S. *Curr. Opin. Struct. Biol.* **2003,** *13*, 284–299.

3. (a) Trauger, J. W., Baird, E. E., and Dervan, P. B. *Nature* **1996,** *382*, 559–561. (b) White, S., Szewczyk, J. W., Turner, J. M., Baird, E. E., and Dervan, P. B. *Nature* **1998,** *391*, 468–470. (c) Kielkopf, C. L., Baird, E. E., Dervan, P. B., and Rees, D. C. *Nat. Struct. Biol.* **1998,** *5*, 104–109. (d) Kielkopf, C. L., White, S., Szewczyk, J. W., Turner, J. M., Baird, E. E., Dervan, P. B., and Rees, D. C. *Science* **1998,** *282*, 111–115.

4. Hsu, C. F., Phillips, J. W., Trauger, J. W., Farkas, M. E., Belitsky, J. M., Heckel, A., Olenyuk, B. Z., Puckett, J. W., Wang, C. C. C., and Dervan, P. B. *Tetrahedron* **2007,** *63*, 6146–6151.

5. (a) Belitsky, J. M., Leslie, S. J., Arora, P. S., Beerman, T. A., and Dervan, P. B. *Bioorg. Med. Chem.* **2002,** *10*, 3313–3318. (b) Crowley, K. S., Phillion, D. P., Woodard, S. S., Scheitzer, B. A., Singh, M., Shabany, H., Burnette, B., Hippenmeyer, P., Heitmeier, M., and Bashkin, J. K. *Bioorg. Med. Chem. Lett.* **2003,** *13*, 1565–1570. (c) Best, T. P., Edelson, B. S., Nickols, N. G., and Dervan, P. B. *Proc. Natl. Acad. Sci. U.S.A.* **2003,** *100*, 12063–12068. (d) Edelson, B. S., Best, T. P., Olenyuk, B., Nickols, N. G., Doss, R. M., Foister, S., Heckel, A., and Dervan, P. B. *Nucleic Acids Res.* **2004,** *32*, 2802–2818. (e) Xiao, X., Yu, P., Lim, H. S., Sikder, D., and Kodadek, T. *Angew. Chem. Int. Ed.* **2007,** *46*, 2865–2868. (f) Nickols, N. G., Jacobs, C. S., Farkas, M. E., and Dervan, P. B. *Nucleic Acids Res.* **2007,** *35*, 363–370. (g) Dose, C., Farkas, M. E., Chenoweth, D. M., and Dervan, P. B. *J. Am. Chem. Soc.* **2008,** *130*, 6859–6866. (h) Hsu, C. F., and Dervan, P. B. *Bioorg. Med. Chem. Lett.* **2008,** *18*, 5851–5855.

6. (a) Gottesfeld, J. M., Melander, C., Suto, R. K., Raviol, H., Luger, K., and Dervan, P. B. Sequence-specific recognition of DNA in the nucleosome by pyrrole-imidazole polyamides. *J. Mol. Biol.* **2001**, *309*, 615–629. (b) Suto, R. K., Edayathumangalam, R. S., White, C. L., Melander, C., Gottesfeld, J. M., Dervan, P. B., and Luger, K. Crystal structures of nucleosome core particles in complex with minor groove DNA-binding ligands. *J. Mol. Biol.* **2003**, *326*, 371–380. (c) Edayathumangalam, R. S., Weyermann, P., Gottesfeld, J. M., Dervan, P. B., and Luger, K. *Proc. Natl. Acad. Sci. U.S.A.* **2004,** *101*, 6864–6869. (d) Dudouet, B., Burnett, R., Dickinson, L. A., Wood, M. R., Melander, C., Belitsky, J. M., Edelson, B., Wurtz, N., Briehn, C., Dervan, P. B., and Gottesfeld, J. M. *Chem. Biol.* **2003,** *10*, 859–867.

7. (a) Olenyuk, B. Z., Zhang, G. J., Klco, J. M., Nickols, N. G., Kaelin, Jr., W. G., and Dervan, P. B. *Proc. Natl. Acad. Sci. U.S.A.* **2004,** *101*, 16768–16773. (b) Kageyama, Y., Sugiyama, H., Ayame, H., Iwai, A., Fujii, Y., Huang, L. E., Kizaka-Kondoh, S., Hiraoka, M., and Kihara, K. *Acta. Oncol.* **2006,** *45*, 317–324. (c) Nickols, N. G., Jacobs, C. S., Farkas, M. E., and Dervan, P. B. *ACS Chem.*

Biol. **2007,** *2*, 561–571.

8. Nickols, N. G., and Dervan, P. B. *Proc. Natl. Acad. Sci. U.S.A.* **2007,** *104*, 10418–10423.

9. (a) Matsuda, H., Fukuda, N., Ueno, T., Tahira, Y., Ayame, H., Zhang, W., Bando, T., Sugiyama, H., Saito, S., Matsumoto, K., and others, O. *J. Am. Soc. Nephrol*. **2006,** *17*, 422–432. (b) Yao, E. H., Fukuda, N., Ueno, T., Matsuda, H., Matsumoto, K., Nagase, H., Matsumoto, Y., Takasaka, A., Serie, K., Sugiyama, H., and Sawamura, T. *Hypertension* **2008**, *52*, 86–92.

10. (a) Cho, J.; Parks, M. E.; Dervan, P. B. *Proc. Natl. Acad. Sci. U.S.A.* **1995**, *92*, 10389–10392. (b) Zhang, Q., Dwyer, T. J., Tsui, V., Case, D. A., Cho, J., Dervan, P. B., Wemmer, D. E. *J. Am. Chem. Soc*. **2004**, *126*, 7958–7966. (c) Herman, D. M., Turner, J. M., Baird, E. E., Dervan, P. B. *J. Am. Chem. Soc*. **1999**, *121*, 1121–1129. (d) Melander, C., Herman, D. M., Dervan, P. B. *Chem. Eur. J*. **2000**, *6*, 4487–4497.

11. Chenoweth D. M., Harki, D. A., and Dervan, P.B. Solution-phase synthesis of pyrrole-imidazole polyamides. *In Press*. (See Chapter 2 of this thesis)

12. (a) Baird, E. E., Dervan, P. B. *J. Am. Chem. Soc*. **1996**, *118*, 6141–6146. (b) Wurtz, N. R., Turner, J. M., Baird, E. E., Dervan, P. B. *Org. Lett*. **2001**, *3*, 1201–1203. (c) Jaramillo, D., Liu, Q., Aldrich-Wright, J., Tor, Y. *J. Org. Chem*. **2004**, *69*, 8151–8153.

13. Trauger, J. W., Dervan P. B. *Methods Enzymol*. **2001**, *340*, 450–466.

14. For examples of polyamides with K_a values $> 2 \times 10^{10}\,\text{M}^{-1}$ and a discussion of the limitations of quantitative DNase I footprint titrations, please refer to reference 5g. An analogous polyamide to **4**, ImPyPyPy-(R)$^{\beta\text{-H}_2\text{N}}\gamma$-ImPyPyPy-$\beta$-Dp, was found to have $K_a > 2 \times 10^{10}\,\text{M}^{-1}$.[5g] Additionally, previous studies with cyclic polyamide cyclo-(-ImPyPyPy-(R)$^{\alpha\text{-H}_2\text{N}}\gamma$-ImPyPyPy-$\gamma$-) found K_a values far exceeding $2 \times 10^{10}\,\text{M}^{-1}$ by DNase I footprint titrations.[10c,d] Cyclic polyamide **1** possesses dual β-amino functionalities; a modification that yields even greater DNA binding affinities compared with α-amino and unsubstituted γ-turns for hairpin polyamides of sequence ImPyPyPy-γ-ImPyPyPy.[5g] The DNA binding affinity of **1** most likely supersedes that of predecessor cyclo-(-ImPyPyPy-(R)$^{\alpha\text{-H}_2\text{N}}\gamma$-ImPyPyPy-$\gamma$-).

15. (a) Pilch, D. S., Poklar, N., Gelfand, C. A., Law, S. M., Breslauer, K. J., Baird, E. E., Dervan, P. B. *Proc. Natl. Acad. Sci. U.S.A.* **1996**, *93*, 8306–8311. (b) Pilch, D. S., Poklar, N., Baird, E. E., Dervan, P. B., Breslauer, K. J. *Biochemistry* **1999**, *38*, 2143–2151.

16. Shaffer, P. L., Jivan, A., Dollins, D. E., Claessens, F., Gewirth, D. T. *Proc. Natl. Acad. Sci. U.S.A.* **2004**, *101*, 4758–4763.

17. For a review of pharmacokinetics in drug discovery see: Ruiz-Garcia, A., Bermejo, M., Moss, A., Casabo, V.G. *J. Pharm. Sci*. **2008**, *97*, 654–690.

18. Apredica, 313 Pleasant St., Watertown, MA 02472 (http://www.apredica.com/).

19. Harki, D. A., Satyamurthy, N., Stout, D. B., Phelps, M. E., Dervan, P. B. *Proc. Natl. Acad. Sci. U.S.A.* **2008**, *105*, 13039–13044.

3.6 Spectra and Supplemental Information
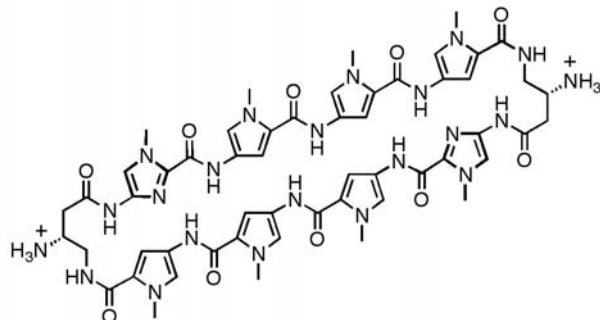
Cyclic polyamide 1

Denoted as **DMC2-239** in ADMET data tables (Table 3.2-3.7) and in full ADMET report located in Appendix B
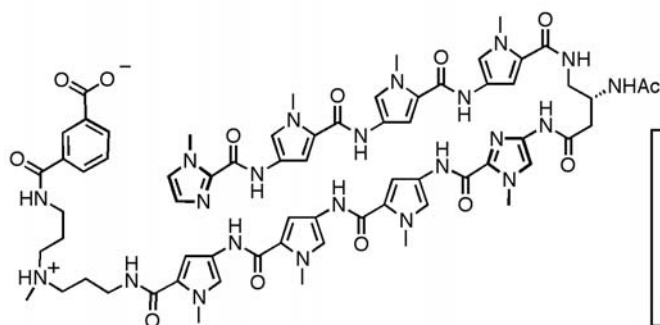
Hairpin polyamide 5

Denoted as **DH-V-88** in ADMET data tables (Table 3.2-3.7) and in full ADMET report located in Appendix B

Figure 3.3 Polyamides **1** and **5** were subjected to preclinical ADMET testing by contract service at Apredica (Watertown, MA). Shown below (Table 3.2-3.7) are summaries of the ADMET results taken directly from the final report provided by Apredica. The full ADMET report, which includes experimental conditions, can be found in Appendix B of this thesis.

Table 3.2 Caco-2 permeability summary from Apredica report (Appendix B).

Client ID	test conc (μM)	Assay duration (hr)	mean A->B P_{app} [a] (10^{-6} cm s^{-1})	mean A->B P_{app} [a] (10^{-6} cm s^{-1})	Asymmetry ratio[b]	comment
Warfarin	50	2	35.4	7.9	0.2	high permeability control
Ranitidine	50	2	1.4	2.4	1.7	low permeability control
DH-V-88	10	2	ND	0.11	UD	
DMC2-239	10	2	ND	ND	ND	

[a]Apparent permeability
[b]P_{app}(B->A) / P_{app}(A->B)
ND = no compound detected in receiver solution

Table 3.3 Cytotoxicity summary from Apredica report (Appendix B).

Client ID	Cell line	IC50 (μM)	comment
Chlorpromazine	HepG2	13	Higly cytotoxic control
Propranolol	HepG2	80	Low cytotoxic control
DH-V-88	HepG2	>100	
DMC2-239	HepG2	>100	

Table 3.4 Fluorescent Cyp IC50 summary from Apredica report (Appendix B).

Client ID	IC$_{50}$ (μM)						
	Cyp1A2 / CEC	Cyp2C8/D BF	Cyp2C9 / DBF	Cyp2C19 / DBF	Cyp2D6 / AMMC	Cyp3A4 / BFC	Cyp3A4 / DBF
Controls	0.2 α-naphtho-flavone	2.3 ketoconazole	1.1 sulpha-phenazole	5.6 tranyl-cypromine	0.05 quinindine	1.26 ketoconazole	1.26 ketoconazole
DH-V-88	>50	>50	>50	>50	>50	47.6	>50
DMC2-239	>50	>50	>50	>50	>50	37.7	>50

Table 3.5 hERG FastPatch summary from Apredica report (Appendix B).

Client ID	IC$_{50}$ (μM)	comment
E-4031	99% at 0.5 μM	positive control
DH-V-88	>100	*
DMC2-239	>100	*

*The solubility limit for this experiment, as determined by vehicle controls, was 17.3 x 10$_3$ LSU (horizontal black line). Based on the data obtained, there may be solubility issues for both test articles at 30 and 100 μM in our physiological saline solution (HB-PS, 0.3%DMSO). Precipitation of DH-V-88 at 100 μM was visible to the naked eye.

Table 3.6 Plasma half-life summary from Apredica report (Appendix B).

Compound	test conc (uM)	medium	T1/2 (min)	Fraction remaining, max time (%)	comment
Propantheline	10.0	Human Plasma	35.5	5.8%	control
Propantheline	10.0	Rat Plasma	149.0	51.6%	control
DH-V-88	10.0	Human Plasma	>120	95.6%	
DH-V-88	10.0	Rat Plasma	>120	94.0%	
DMC2-239	10.0	Human Plasma	>120	124.5%	
DMC2-239	10.0	Rat Plasma	>120	120.3%	

[a]Half-life

Table 3.7 Plasma protein binding summary from Apredica report (Appendix B).

Client ID	test conc (μM)	Assay duration	Species	Mean free fraction (%)	comment
Warfarin	10	4 hr	Human	0.73%	high binding control
Warfarin	10	4 hr	Rat	5.47%	high binding control
Atenolol	10	4 hr	Human	76.2%	low binding control
Atenolol	10	4 hr	Rat	84.7%	low binding control
DH-V-88	10	4 hr	Human	0.0015%	
DH-V-88	10	4 hr	Rat	0.0016%	
DMC2-239	10	4 hr	Human	0.0000%	
DMC2-239	10	4 hr	Rat	0.0040%	

ppm

NHBoc

NHCbz

O

H
N

N

N

HO₂C

exp1 Proton

SAMPLE   SPECIAL
date   Oct 21 2008   temp   23.0
solvent   dmso   gain   not used
file /home/autouse~ spin   not used
r/vnmrsys/data/aut~ hst   0.008
o_2008.10.19/s_200~ pw90   9.900
8i020_22/data/Prot~ alfa   6.600
        on_01.fid
    ACQUISITION   FLAGS
sw   8000.0   il   n
at   2.048   in   n
np   32762   dp   y
fb   not used   hs   nn
bs   32   PROCESSING
ss   2   lb   0.20
d1   1.000   fn   65536
nt   64   DISPLAY
ct   64   sp   -3.9
    TRANSMITTER   wp   5999.8
tn   H1   rfl   2248.3
sfrq   499.772   rfp   1244.4
tof   499.6   rp   41.8
tpwr   61   lp   7.6
pw   4.950   PLOT
    DECOUPLER   wc   240
dn   C13   sc   0
dof   0   vs   50
dm   nnn   th   6
dmm   c   ai   cdc ph
dpwr   35
dmf   32258

Figure 3.4 ¹H NMR BocHN-(*R*)^β-CbzHN^γ-Im-CO₂H (**8**)
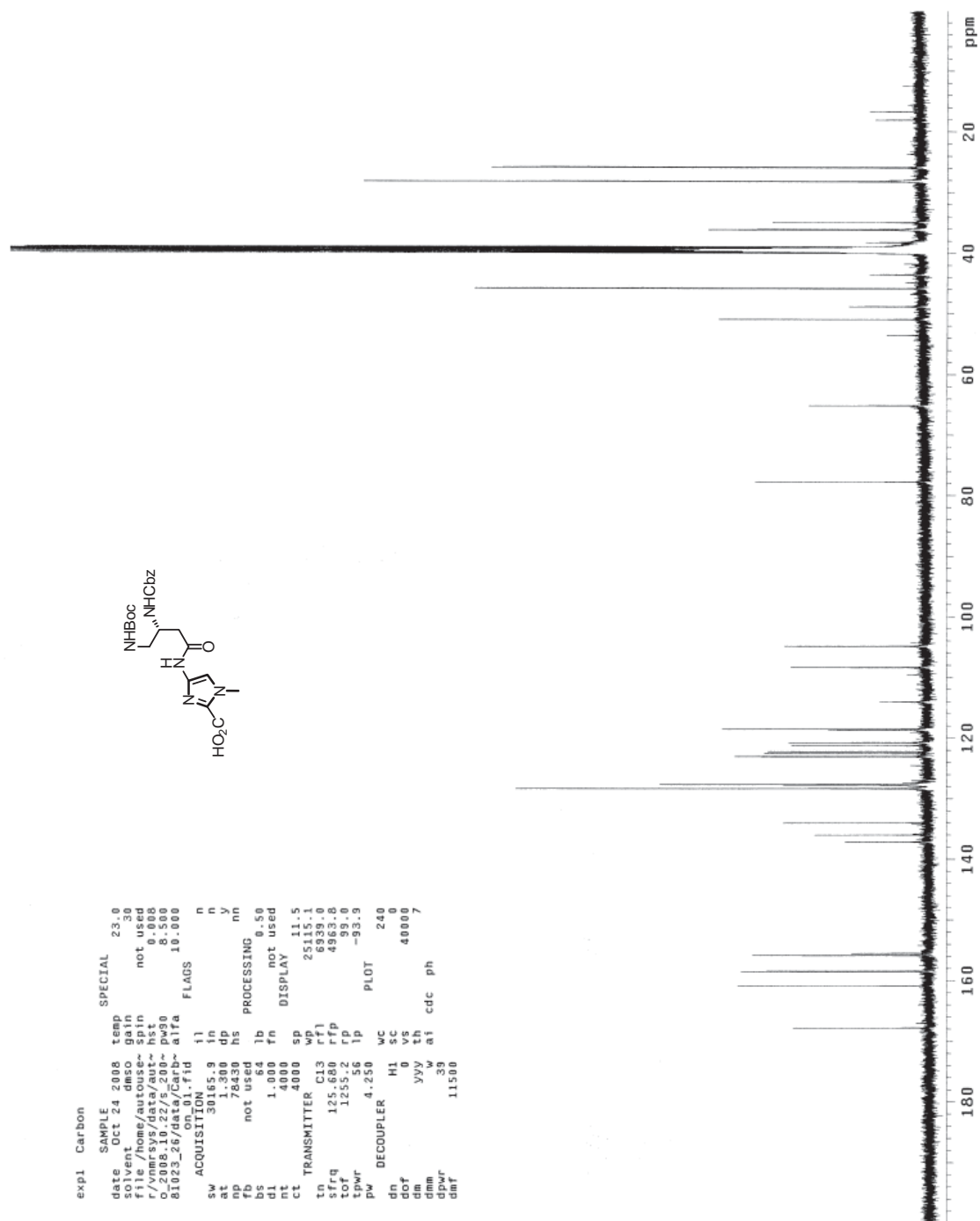
Figure 3.5 ^{13}C NMR BocHN-(*R*)[β-CbzHN]γ-Im-CO$_2$H (**8**)
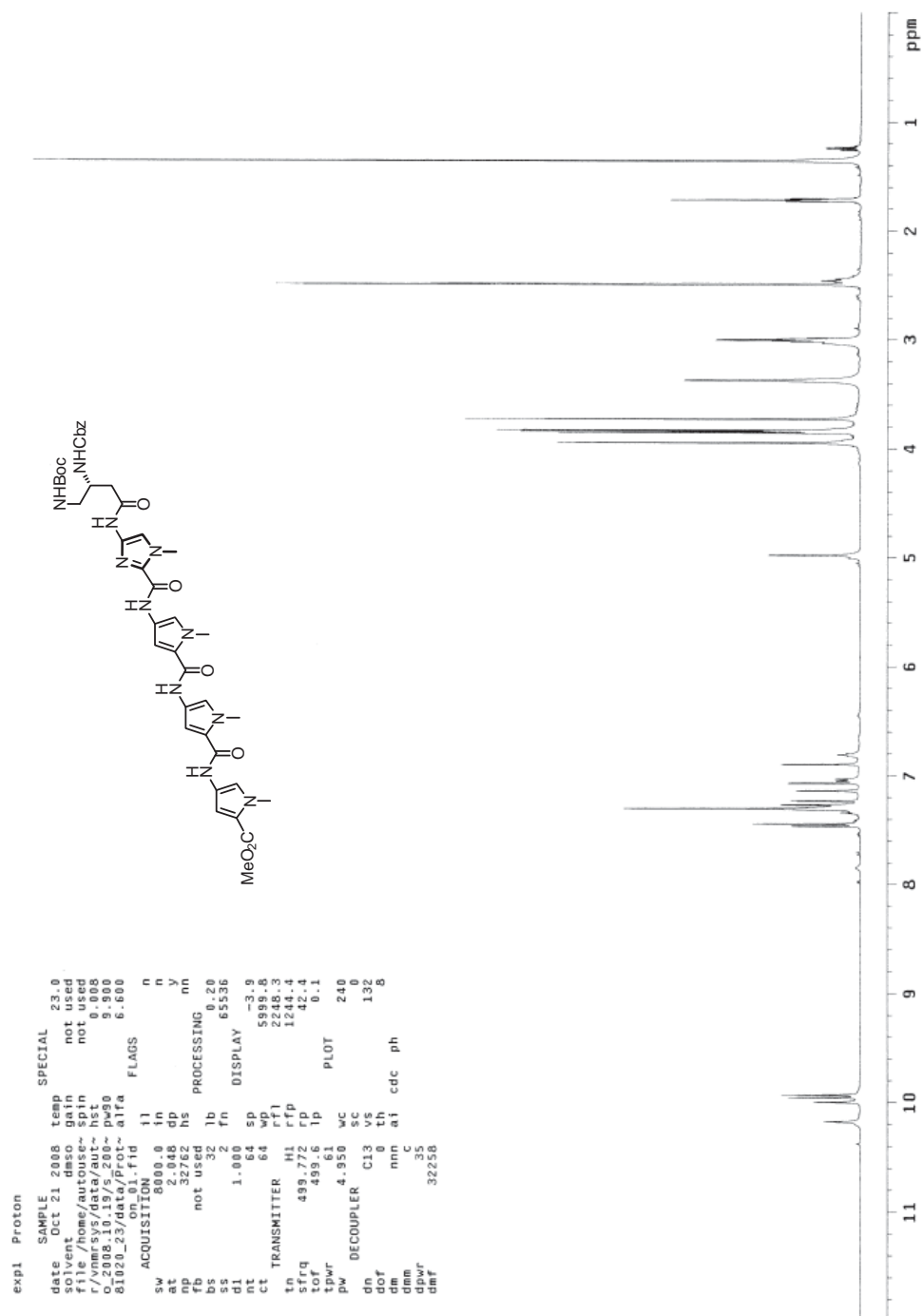
Figure 3.6 ^{1}H NMR BocHN-(*R*)$^{\beta\text{-CbzHN}}\gamma$-ImPyPyPy-CO$_2$Me (**9**)

Figure 3.7 ^{13}C NMR BocHN-(R)$^{\beta\text{-CbzHN}}\gamma$-ImPyPyPy-CO$_2$Me (**9**)
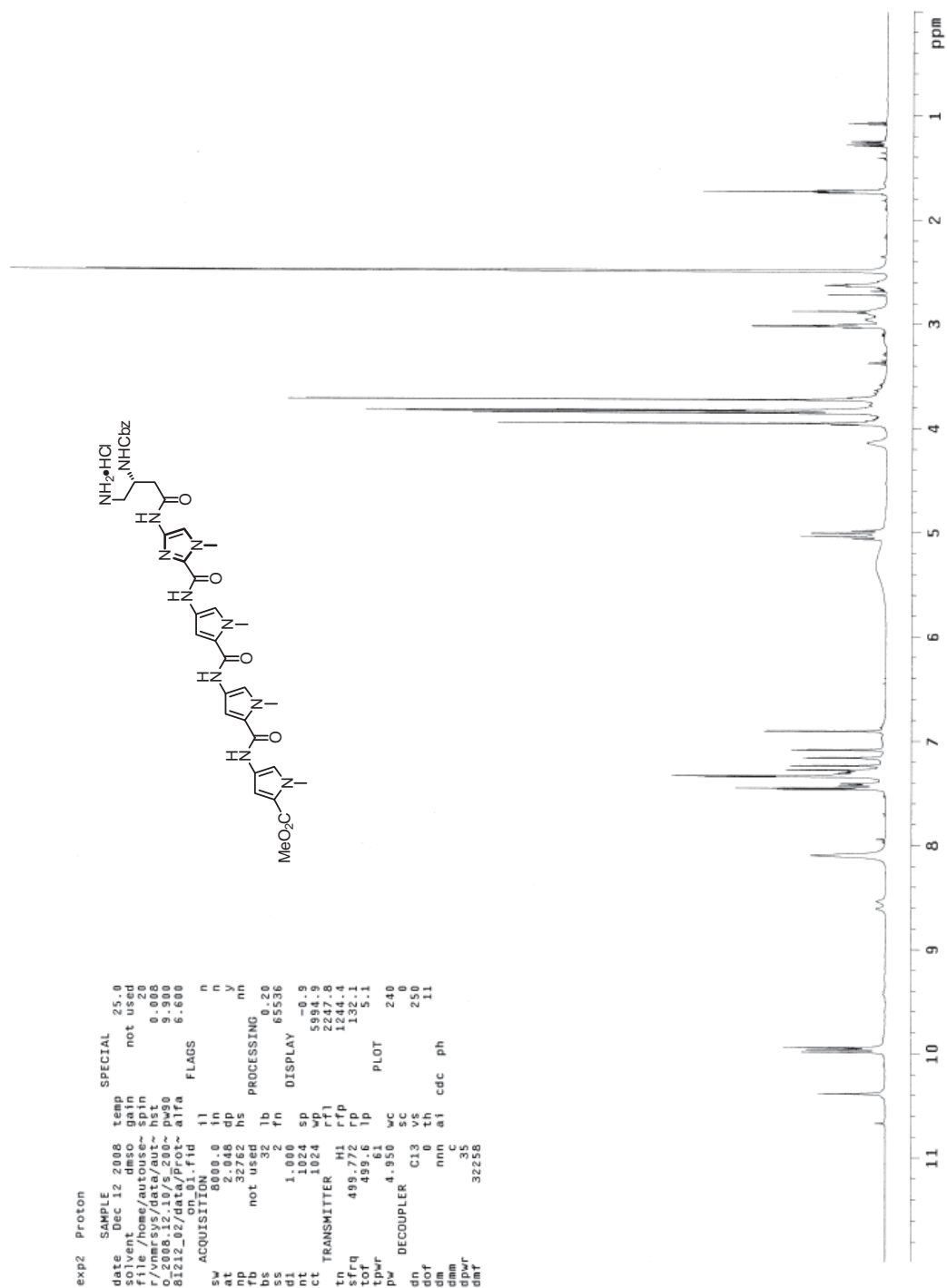
Figure 3.8 ^{1}H NMR HCl•H$_2$N-(*R*)$^{\beta\text{-CbzHN}}\gamma$-ImPyPyPy-CO$_2$Me (**10**)
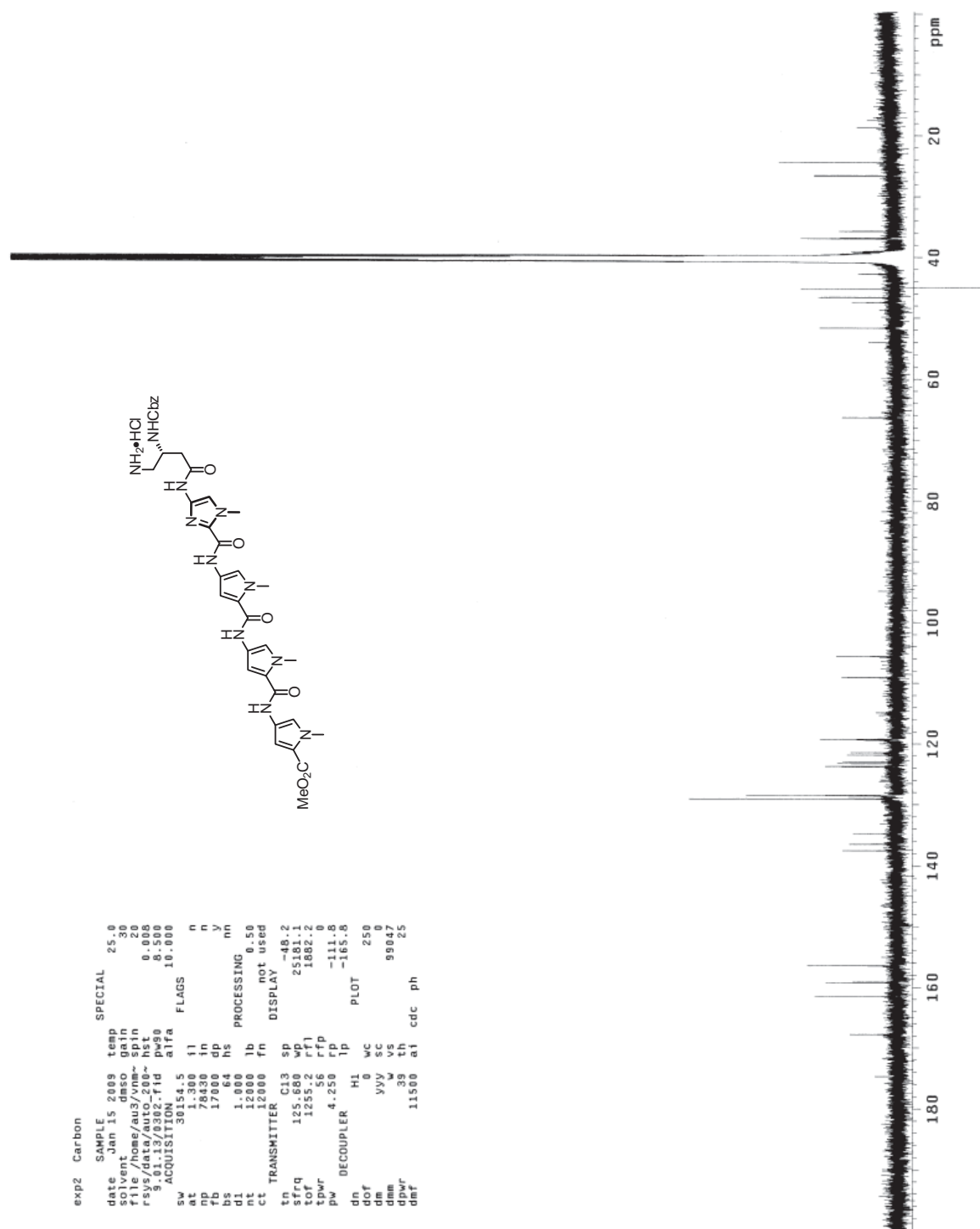
Figure 3.9 ^{13}C NMR HCl•H$_2$N-(R)$^{\beta\text{-CbzHN}}\gamma$-ImPyPyPy-CO$_2$Me (**10**)

Figure 3.10 ^{1}H NMR BocHN-$(R)^{\beta\text{-CbzHN}}\gamma$-ImPyPyPy-CO$_2$H (**11**)

Figure 3.11 ^{13}C NMR BocHN-(*R*)[β-CbzHN]γ-ImPyPyPy-CO$_2$H (**11**)
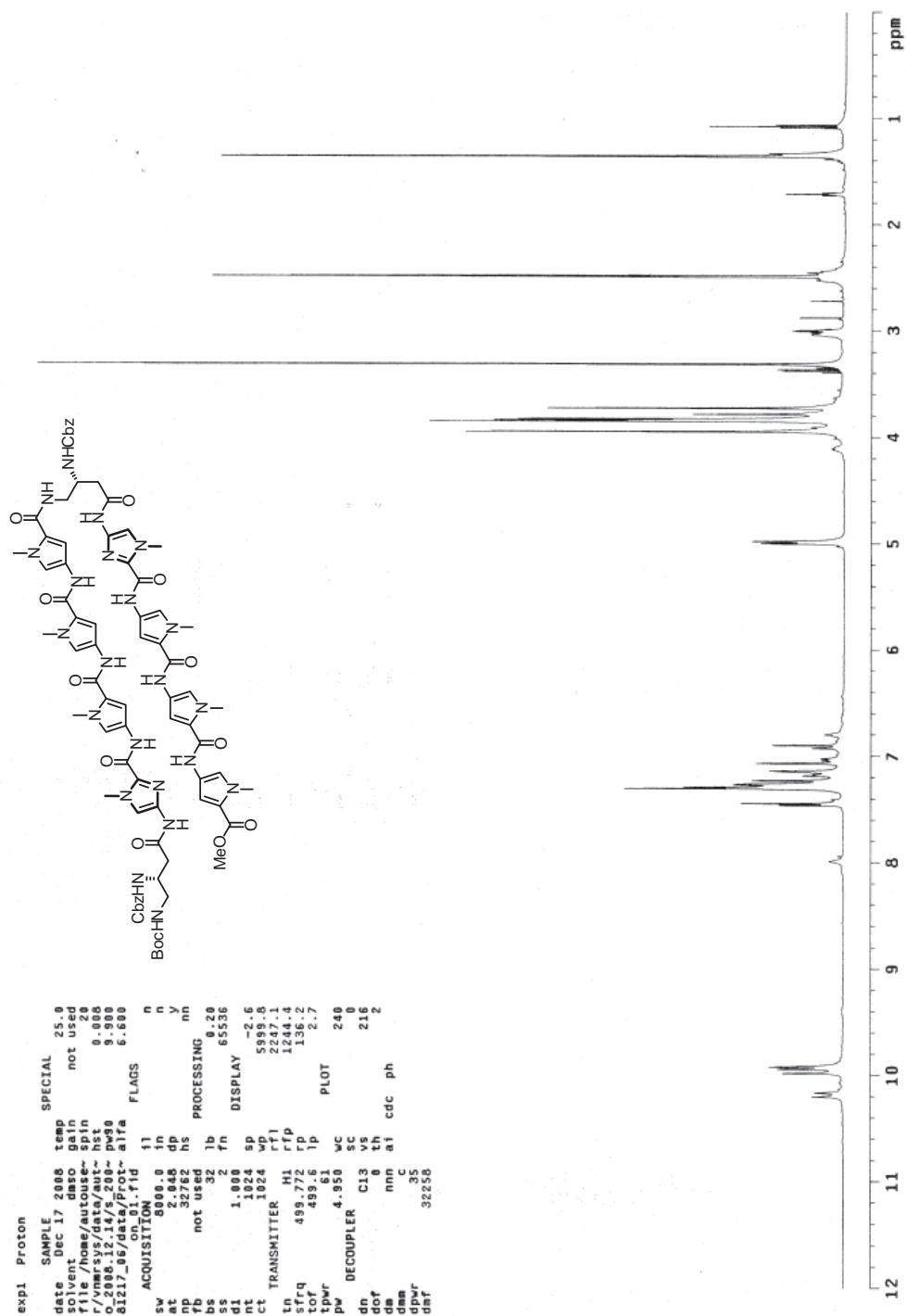
Figure 3.12 ¹H NMR BocHN-(*R*)[β-CbzHN]γ-ImPyPyPy-(*R*)[β-CbzHN]γ-ImPyPyPy-CO$_2$Me (**12**)
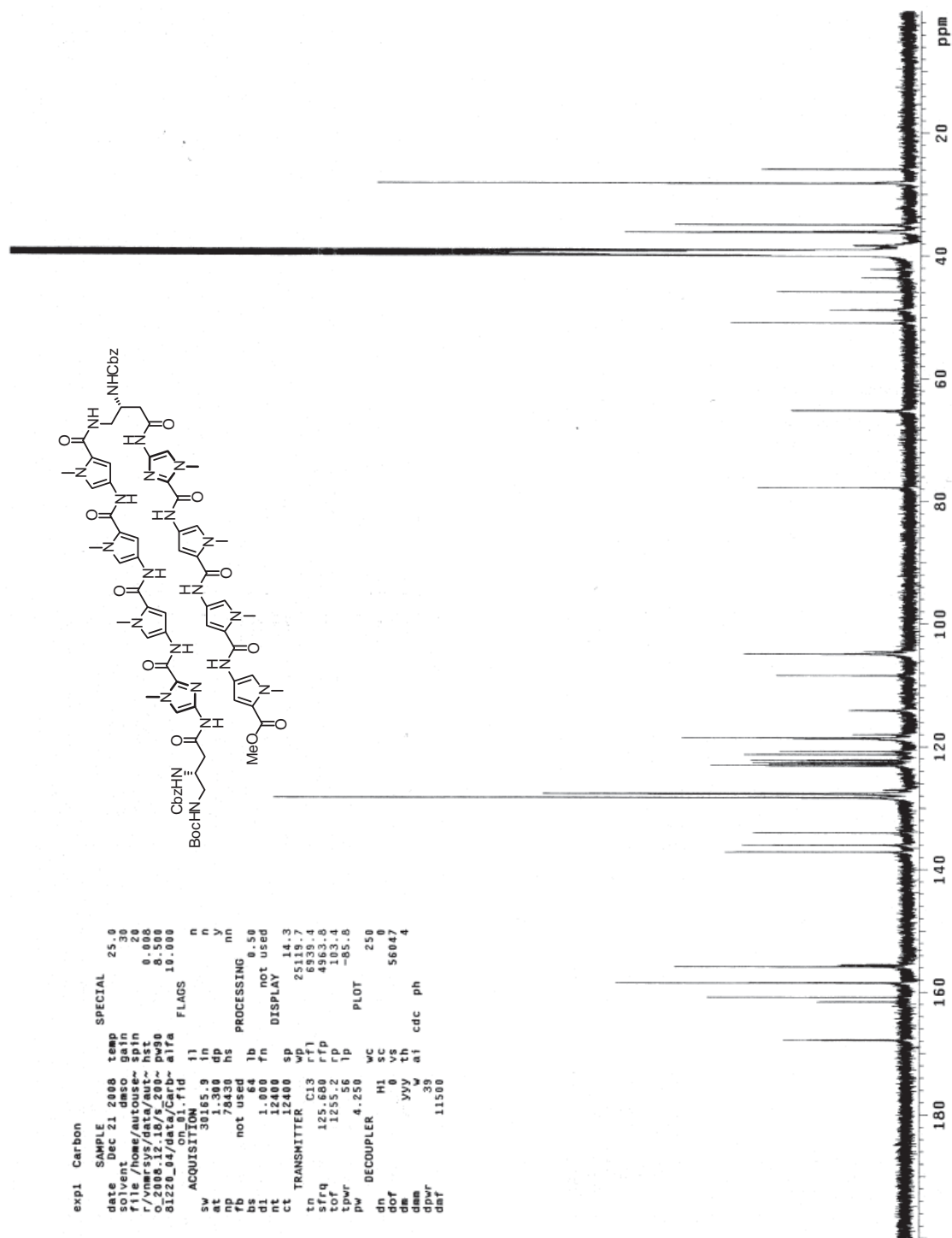
Figure 3.13 ^{13}C NMR BocHN-(*R*)$^{\beta\text{-CbzHN}}\gamma$-ImPyPyPy-(*R*)$^{\beta\text{-CbzHN}}\gamma$-ImPyPyPy-CO$_2$Me (**12**)

Figure 3.14 ^{1}H NMR BocHN-(*R*)$^{\beta\text{-CbzHN}}\gamma$-ImPyPyPy-(*R*)$^{\beta\text{-CbzHN}}\gamma$-ImPyPyPy-CO$_2$H (**13**)

Figure 3.15 ^{13}C NMR BocHN-(R)$^{\beta\text{-CbzHN}}\gamma$-ImPyPyPy-($R$)$^{\beta\text{-CbzHN}}\gamma$-ImPyPyPy-CO$_2$H (**13**)
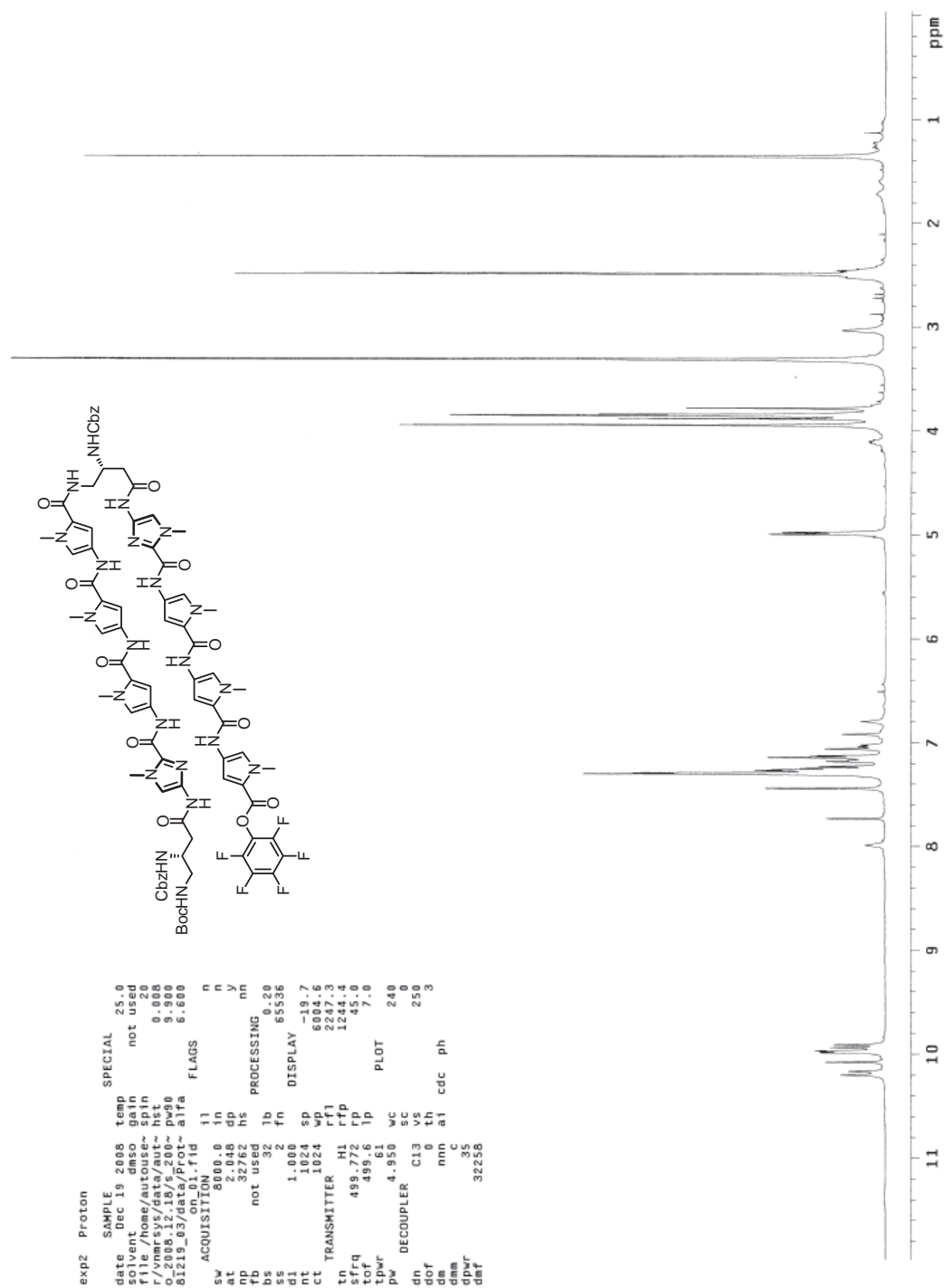
Figure 3.16 ^{1}H NMR BocHN-(R)$^{\beta\text{-CbzHN}}\gamma$-ImPyPyPy-($R$)$^{\beta\text{-CbzHN}}\gamma$-ImPyPyPy-CO$_2$Pfp (**14**)

ppm

(CF$_3$CO$_2$H salt)

$^+$NH$_3$

H$_3$N$^+$

exp3 Proton

SAMPLE
date   Jan 20 2009
solvent   dmso
file /home/au3/vnm~
rsys/data/auto-200~
9.01.19/3201.fid
ACQUISITION
sw   8000.0
at   2.048
np   32762
fb   not used
bs   32
ss   2
d1   1.000
nt   800
ct   800

TRANSMITTER   H1
tn
sfrq   499.772
tof   499.6
tpwr   61
pw   4.950

DECOUPLER   C13
dn   0
dof
dm   nnn
dmm   c
dpwr   35
dmf   32258

temp   25.0
gain   not used
spin   20
hst   0.008
pw90   9.900
alfa   6.600

FLAGS
il   n
in   n
dp   y
hs   nn

PROCESSING
lb   0.20
fn   65536

DISPLAY
sp   -8.0
wp   6008.8
rfl   2248.0
rfp   1244.4
rp   142.2
lp   -0.2

PLOT
wc   250
sc   0
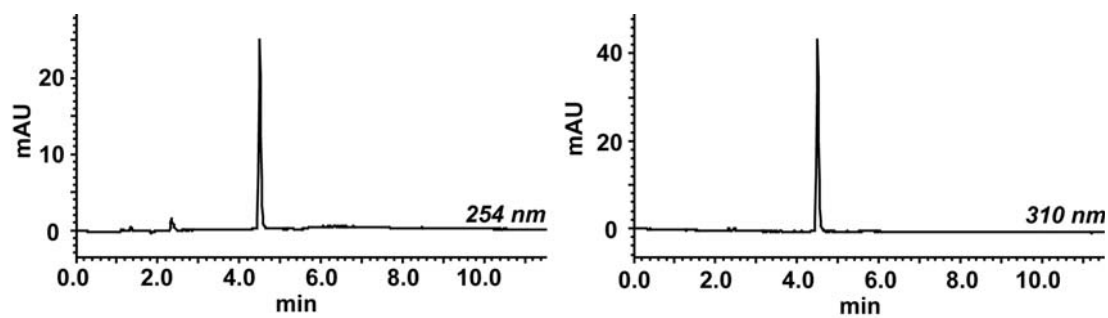vs   1009
th   1
ai   cdc ph

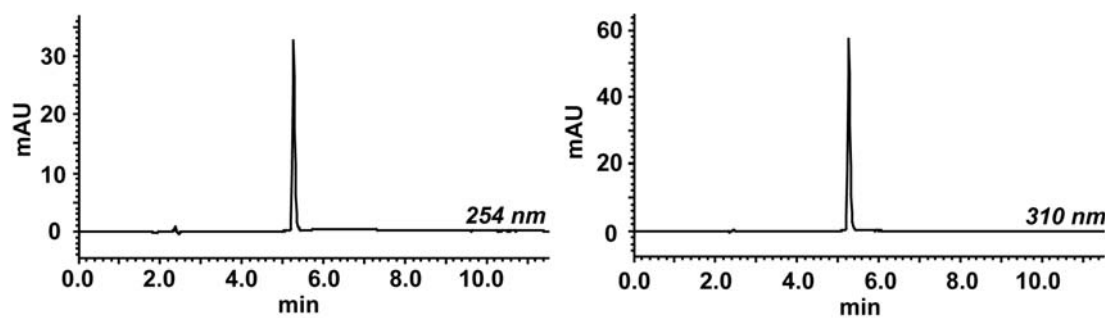**Figure 3.17** ^{1}H NMR *cyclo*-(-ImPyPyPy-(*R*)$^{β-H2N}$γ-ImPyPyPy-(*R*)$^{β-H2N}$γ-) (**1**)
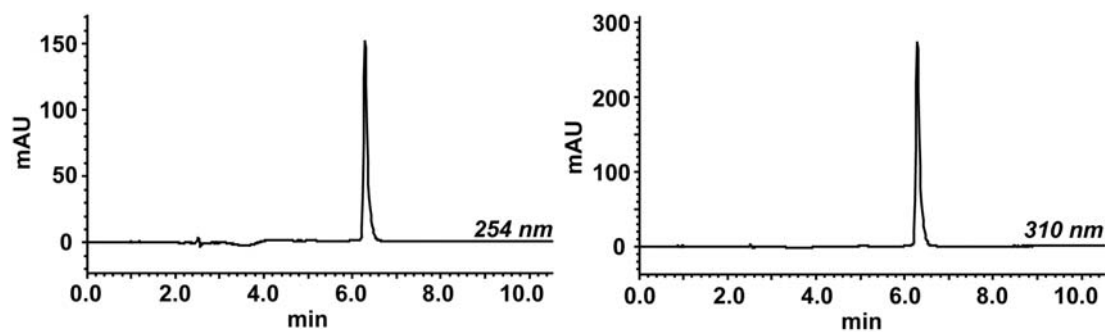
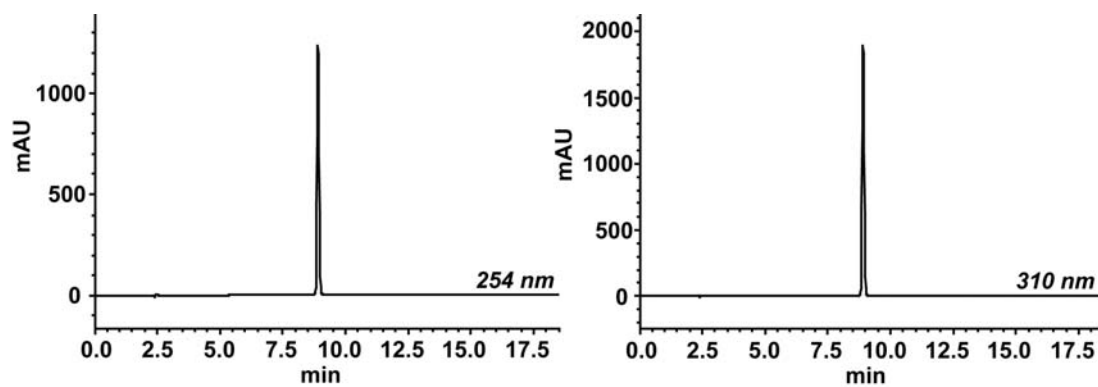**Figure 3.18** Analytical HPLC characterization of cyclic polyamide **15**.
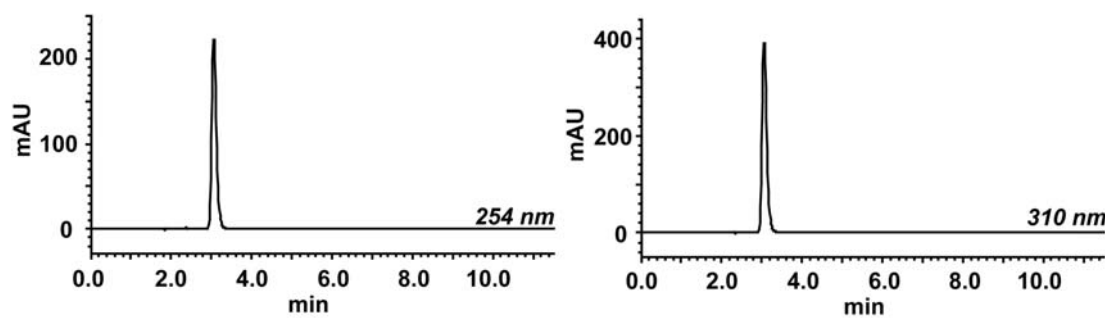
Figure 3.19 Analytical HPLC characterization of cyclic polyamide **1**.

Figure 3.20 Analytical HPLC characterization of cyclic polyamide **3**.

Figure 3.21 Analytical HPLC characterization of cyclic polyamide **2**.

Figure 3.22 Analytical HPLC characterization of cyclic polyamide **5**.